Brain, Behavior, and Immunity 87 (2020) 634–644

Contents lists available at ScienceDirect

Brain, Behavior, and Immunity

journal homepage: www.elsevier.com/locate/ybrbi

Decreased IL-1β-induced CCL20 response in human iPSC-astrocytes in schizophrenia: Potential attenuating effects on recruitment of regulatory T cells

Ibrahim A. Akkouh[a,b], Thor Ueland[a,c,d], Lars Hansson[a,b], Elin Inderhaug[a,b], Timothy Hughes[a,b], Nils Eiel Steen[a], Pål Aukrust[d,e,f,g], Ole A. Andreassen[a], Attila Szabo[a,b,*,1], Srdjan Djurovic[b,h,*,1]

[a] NORMENT, Institute of Clinical Medicine, University of Oslo, and Division of Mental Health and Addiction, Oslo University Hospital, Oslo, Norway
[b] Department of Medical Genetics, Oslo University Hospital, Oslo, Norway
[c] Research Institute of Internal Medicine, Oslo University Hospital Rikshospitalet, Oslo, Norway
[d] K.G. Jebsen-Thrombosis Research and Expertise Center (TREC), University of Tromsø, Tromsø, Norway
[e] Research Institute of Internal Medicine, Oslo University Hospital Rikshospitalet, Oslo, Norway
[f] Section of Clinical Immunology and Infectious Diseases, Oslo University Hospital, Rikshospitalet, Norway
[g] K.G. Jebsen Inflammatory Research Center, University of Oslo, Norway
[h] NORMENT, Department of Clinical Science, University of Bergen, Bergen, Norway

ARTICLE INFO

Keywords:
Schizophrenia
iPSC
Astrocyte
Inflammation
CCL20
Regulatory T cell
RNA-sequencing

ABSTRACT

Schizophrenia (SCZ) is a severe mental disorder with a high heritability. Although its pathophysiology is mainly unknown, dysregulated immune activation and inflammation have recently emerged as possible candidates in the underlying mechanisms of SCZ. Previous studies suggest that aberrant inflammasome activation, glia dysregulation, and brain inflammation may be involved in the pathophysiology of the disorder. Here, we studied the effects of inflammatory modulation on human induced pluripotent stem cell (iPSC)-derived astrocytes generated from SCZ patients and healthy controls (CTRL). Inflammasome activation was mimicked by short-term IL-1β exposure, and gene expression were measured with high-coverage RNA-Seq to ensure a global characterization of the transcriptional effects of the treatment. IL-1β exposure modulated several pathways involved in innate immune responses, cell cycle regulation, and metabolism in both SCZ and CTRL astrocytes. Significant differences were found in the expression of *HILPDA* and *CCL20* genes, both of which had reduced up-regulation upon IL-1β treatment in SCZ astrocytes compared to CTRL astrocytes. CCL20 data were further validated and confirmed using qPCR, ELISA, and regulatory T lymphocyte (T_{reg}) migration assays. Additionally, we found significantly decreased mRNA expression of the T_{reg}-specific marker FOXP3 in the blood of a large cohort of SCZ patients (n = 484) compared to CTRL (n = 472). Since CCL20 is a specific chemoattractant for $CD4^+CD25^+CCR6^+$ T_{regs}, which are crucially involved in anti-inflammatory responses during brain (auto)inflammation, our results imply a plausible role for an altered astroglia-CCL20-CCR6-T_{reg} axis in SCZ pathophysiology.

1. Introduction

Schizophrenia (SCZ) is a severe mental disorder that poses a considerable burden on the affected individuals, with high impact on morbidity and mortality, life quality, and costs of patient care worldwide (Correll, 2015). Although it has high heritability, the details of its patophysiology and etiology are still unknown. This gap of knowledge hampers the treatment of patients as the identification of the underlying disease mechanisms in SCZ is essential for developing effective new treatment regimens (Editorial, 2010; Rubinstein, 2010). Genome-wide association studies (GWAS) have identified robust genetic associations with SCZ in immune-related regions of the genome (DeLisi, 2002; Irish Schizophrenia Genomics Consortium and the Wellcome Trust Case Control Consortium 2, 2012; Corvin and Morris, 2014;

* Corresponding authors at: NORMENT, Institute of Clinical Medicine, University of Oslo, and Division of Mental Health and Addiction, Oslo University Hospital, Building 49, P.O. box 4956 Nydalen, Oslo 0424, Norway (A. Szabo). Department of Medical Genetics, Oslo University Hospital, Building 25, Kirkeveien 166, 0450 Oslo, Norway (S. Djurovic).
E-mail addresses: attila.szabo@medisin.uio.no (A. Szabo), srdjan.djurovic@medisin.uio.no (S. Djurovic).
[1] These authors share senior authorship.

https://doi.org/10.1016/j.bbi.2020.02.008
Received 10 September 2019; Received in revised form 16 January 2020; Accepted 20 February 2020
Available online 25 February 2020

Table 1
Demographic characteristics of schizophrenia (SCZ) and healthy (CTRL) fibroblast donors participated in this study.

	SCZ			CTRL		
	donor 1	donor 2	donor 3	donor 1	donor 2	donor 3
Age at biopsy	23	27	20	33	38	46
Sex	male	female	male	female	male	female
Ethnicity	Caucasian	Caucasian	Caucasian	Caucasian	Caucasian	Caucasian

International Schizophrenia Consortium et al., 2009; Schizophrenia Working Group of the Psychiatric Genomics Consortium, 2014). Dysregulated immune activation and inflammation could be involved in the pathophysiology and represent an underlying mechanism explaining different SCZ symptoms (Khandaker, 2015; Miyaoka, 2017). Indeed, autoimmunity, infections, and CNS inflammation may play a role in the manifestation of the disease (Bechter, 2010; Benros, 2011). Recent studies suggest a role of neuroinflammation in SCZ as a result of dysregulated glia functions, and have linked endothelial cell activation and systemic inflammatory markers to brain pathology (Najjar and Pearlman, 2015; Dieset, 2015). Furthermore, elevated circulating levels of inflammatory markers (e.g. interleukin [IL]-1 receptor antagonist [IL-1Ra] and soluble tumor necrosis factor receptor type 1 [TNF-R1]) were shown to be associated with disease severity in SCZ, (Hope, 2013) but the potential pathophysiological role of inflammation in SCZ is still not clear.

Astroglia and microglia are resident immunocompetent cells of the mammalian brain, (Heneka, 2018) and are potential candidates for immune-abnormalities in SCZ (Khandaker, 2015). Recent studies in astrocytes isolated from human postmortem samples and experimental models indicate a plethora of changes in neuropsychiatric disorders. These include decreased astrocyte cellular features and gene expression in depression, chronic stress and anxiety, and, notably, increased inflammation in SCZ (Kim, 2018). Neuroinflammation may be a consequence of dysregulated innate immune responses in the CNS against various microbial, chemical, or physical insults evoked by exogenous or endogenous danger signals. Inflammasomes, in particular NLRP3 inflammasomes, are an important part of innate immune responses where activated caspase 1 cleaves the proforms of the inflammatory cytokines IL-1β and IL-18 into their active and released forms (Heneka, 2018; Singhal, 2014; Swanson et al., 2019). These cytokines play a critical role in the activation of various down-stream inflammatory pathways, and have also been suggested to be involved in psychiatric disorders, such as SCZ, as a consequence of their dysregulated secretion by microglia and other brain-resident immune cells (Khandaker, 2015). Elevated serum and postmortem brain IL-1β levels have been associated with symptom severity and disease progression in SCZ (Zhu, 2018; Mohammadi, 2018). Furthermore, abnormal inflammatory astrocyte functions have recently been related to cognitive impairment and brain volume reduction in SCZ (Kindler, et al., 2019).

There is, however, sparse direct evidence for immune pathology due to the inaccessibility to human CNS tissue and the lack of appropriate animal models of SCZ. Recent method developments in human iPSC biology have enabled studies to elucidate cellular and molecular anomalies in SCZ (Windrem, 2017; Falk, 2016). Direct reprogramming of fibroblasts into iPSCs and their subsequent, controlled differentiation to iPSC-neurons has been demonstrated to be a feasible model for investigating the molecular pathology of SCZ (Brennand, 2011; Tran, 2013). Here, we study the effects of inflammatory modulation on human iPSC-derived astrocytes generated from SCZ patients and healthy controls by using IL-1β as a prototypical and relevant inflammatory stimulus.

2. Materials and methods

2.1. Recruitment of patients and collection of skin biopsies

This project is part of the ongoing Norwegian TOP (Thematically Organized Psychosis) study. Information about recruitment procedures, inclusion and exclusion criteria, and clinical assessments for the TOP study as a whole have been described in detail (Morch, 2019; Simonsen, 2011). For reprogramming and astrocyte differentiation, fibroblast/skin biopsies were isolated from 3 CTRLs and 3 SCZ patients that were selected based on clinical information. For gene expression measurements of T_{reg} markers in whole blood, a subset of the TOP sample consisting of 484 SCZ spectrum disorder patients (353 schizophrenia, 41 schizophreniform, and 90 schizoaffective) and 472 CTRL subjects was used. These participants were selected based on the availability of microarray gene expression data for the relevant markers. A detailed description of blood sampling procedures, microarray pre-processing, and quality control can be found in a previous report (Akkouh, 2018). Tables 1 and 2 show further details about the study participants from whom skin biopsies and whole blood samples were obtained, respectively. All patients underwent a clinical examination that included diagnostic interviews based on Structured Clinical Interview in DSM-IV axis I Disorders (SCID-1) and structured assessments of clinical symptoms, use of psychotropic medication, smoking habits, alcohol consumption, and illicit substance use. Diagnostic evaluation was performed by trained clinical psychologists and psychiatrists. The main inclusion criteria were confirmed diagnosis of SCZ according to the Diagnostic and Statistical manual of Mental Disorders (DSM)-IV, age between 18 and 65, and ability to give informed written consent. The main exclusion criteria were clinically significant brain injury, neurological disorder, ongoing infections, autoimmune disorders or any form of cancer. All participants have given written consent and the study was approved by the Norwegian Scientific Ethical Committees and the Norwegian Data Protection Agency. The project has been approved by the Regional Ethics Committee of the South-Eastern Norway Regional Health Authority (REK grant: #2012/2204 “Bruk av stamceller for å skaffe kunnskap om sykdomsmekanismer ved alvorlige psykiske lidelser.”). The authors assert that all procedures contributing to this work comply with the ethical standards of relevant guidelines and regulations.

Table 2
Demographic and clinical characteristics of SCZ and CTRL subjects used for gene expression measurements in whole blood.

	SCZ (n = 484)		CTRL (n = 472)			
	Mean	SD	Mean	SD	Test statistic	p-value
Age	30.5	9.5	32.3	8.5	t = −3.10	1.99e-3*
Sex, female (n, %)	189	39.0	209	44.3	$\chi 2$ = 0.84	0.36
Education (years)	14.7	44.9	14.5	2.2	t = 0.13	0.89

*p < 0.05.

2.2. Generation and maintenance of hiPSCs

Fibroblasts isolated from control and patient donors were grown and expanded *in vitro* in DMEM containing 10% fetal bovine serum, 1% penicillin/streptomycin, and 1% Glutamax. Cells were reprogrammed using Sendai virus, transduced with the CytoTune™-iPS 2.0 Sendai Reprogramming Kit (Thermo Fisher, Waltham, MA, USA) containing KOS (Klf4, Oct4, Sox2), Nanog, and c-Myc reprogramming factors. Virus vector was washed out after 24 h. At day 7 after transduction, cells were plated on Vitronectin and medium was changed to Essential 8 Flex Medium (Thermo Fisher). Passaging of iPSC was done at a maximum of 80% confluency or every 3–4 days by using 0.5 mM EDTA for 3–5 min at 37 °C. Cells were split in 1:3 ratio on Geltrex coated plates in the presence of 10 μM ROCK inhibitor Y27632 (Miltenyi Biotec, Bergisch Gladbach, Germany). Complete elimination of virus was corroborated in iPSCs at passage 10 by qPCR with specific SeV genome detection primers (TaqMan Mr04269880-mr; Thermo Fisher). Each iPSC line was subjected to rigorous quality control at The Norwegian Center for Stem Cell Research including phenotyping, regular monitoring of morphology, and pluripotency marker expressions. Karyotyping examination of the chromosomal integrity of all the derived iPSC lines was performed at passage 15 for verification of authenticity and normality (KaryoStat Karyotyping Service, Thermo Fisher). Karyotyping test results and hiPSC phenotyping data that are not included in this paper are available upon request.

2.3. Differentiation of astrocytes from donor iPSCs

We differentiated astrocytes from patient and control iPSCs following previously published glial differentiation protocols with small modifications (Izrael, 2007; Tcw, 2017). Briefly, iPSC colonies at passages 24–25 were transferred to 6-well tissue culture plates in Neural maintenance medium (NMM) consisting of 50% DMEM/F12 and 50% Neurobasal medium (both from Thermo Fisher) supplemented with 0.5% (v/v) N2, 1% (v/v) B27 (both from Invitrogen, Carlsbad, CA, USA), 5 μg/ml human insulin, 40 ng/ml triiodothyronine (T3), 10 μM β-mercaptoethanol, 1.5 mM L-glutamine, 100 μM NEAA, 100 U/ml penicillin and 100 μg/ml streptomycin (all from Sigma-Aldrich, St. Louis, MO, USA). 20 ng/ml EGF and 4 ng/ml bFGF (both from Peprotech, Rocky Hill, NJ, USA) were added to the cultures. After 1 day, non-adherent embryoid bodies (EBs) formed in the cultures and were fed daily with NMM containing T3, EGF and bFGF (as above) until day 3 (Fig. 1B). On day 3, 10 μM all-trans retinoic acid (ATRA, Sigma) was added to the medium and EBs were washed (1x, gently in NMM medium) and plated on Geltrex-coated plates (Thermo Fisher). After this step, cultures were fed with 10 μM ATRA + T3 + EGF + bFGF supplemented NMM medium daily until day 10 (Fig. 1B). In order to avoid the disruption of neurorosettes, cultures were not splitted until day 10. On day 10, neurorosette formation was monitored by light microscopy, and *Nestin* and *PAX6* positivity was checked by qPCR. Cultures were passaged using the cell dissociation agent Accutase (Sigma) following the recommended protocol. From this point on, regular passaging was done at confluence and cultures were seeded on Geltrex-coated 6-well plates. On day 10, the medium was changed to NMM + 40 ng/ml T3 + 20 ng/ml EGF. On day 18, after the formation of neuroepithelium, the medium was changed to NMM supplemented with B27 without vitamin A (Invitrogen) + 20 ng/ml EGF + 40 ng/ml T3, and cultures were fed using the same medium composition until day 42. For astrocyte maturation and enrichment, medium was switched to ScienCell AM medium (ScienCell, Carlsbad, CA, USA) on day 42, and cells were further cultured for 60 additional days until day 102. Cultures were continuously biobanked from day 42 by freezing astrocytes in Sciencell AM medium + 10% DMSO at each passage, and storing them in liquid nitrogen. Samples were continuously collected during the differentiation process at days 0 (iPSC), 7, 14, 21, 30, and 40. The mRNA expression of *PAX6*, *Nestin*, and the astrocyte-specific markers *GFAP*, *S100B*, *SLC1A2*, *SLC1A3*, *FABP7*, *AQP4*, *ALDH1L1*, and *ALDOC* was monitored by qPCR using a custom-made TLDA gene array card (Thermo Fisher). Cells were stained with anti-GFAP, anti-MAP2 and anti-NG2 antibodies (all from Abcam, Cambridge, UK) and were analyzed using fluorescent microscopy on day 42 (GFAP) and day 102 (GFAP, S100B, and AQP4, and GFAP, MAP2, NG2 co-staining). Astrocytes were considered mature and were used for experiments from day 102.

2.4. Inflammatory modulation of mature astrocytes

To mimic inflammasome activation *in vitro*, day 102 astrocytes were treated with IL-1β at working concentrations of 0.1–10 ng/ml (Peprotech). Cell pellets and culture supernatants were collected after 4 h of incubation for RNA-Seq and qPCR, and after 24 h of incubation for ELISA and migration assay. Harvested samples were either immediately used for analyses, or stored at −80 °C.

2.5. RNA extraction and sequencing

Total RNA was extracted from the differentiated astrocyte samples using either the RNeasy Plus Mini Kit (Qiagen, Hilden, Germany) or the MagMax mirVana Total RNA Isolation Kit (Thermo Fisher) according to manufacturer's instructions. In both cases, approximately 1 million cells were used as input. RNA yield was quantified with a NanoDrop 8000 Spectrophotometer (NanoDrop Technologies, Wilmington, DE, USA) and RNA integrity was assessed with Bioanalyzer 2100 RNA 6000 Nano Kit (Agilent Technologies, Santa Clara, CA, USA). All samples had an RNA Integrity Number (RIN) > 8. Library preparation and paired-end RNA-sequencing were carried out at the Norwegian High-Throughput Sequencing Centre (www.sequencing.uio.no). Briefly, libraries were prepared with the TruSeq Stranded mRNA kit from Illumina (San Diego, CA, USA) which involves Poly-A purification to capture coding as well as several non-coding RNAs. The prepared samples were then sequenced on a HiSeq 4000 sequencer (Illumina) at an average depth of 50 million reads per sample using a read length of 150 base pairs and an insert size of 350 base pairs.

2.6. qPCR/TLDA array

cDNA was generated from 500 ng of total RNA, using the High-Capacity cDNA Reverse Transcription Kit (Cat No. 4368813, Life Technologies Corporation, Carlsbad, CA, USA) according to the manufacturer's protocol.

qPCR was performed with custom designed TaqMan low density array (TLDA) cards (Life Technologies; catalog numbers of the included TaqMan probes are available upon request). Briefly, 100 ng of cDNA was loaded per port according to the manufacturer's protocol. The cards were then cycled and analyzed on a Quantstudio 12 K Flex Real-Time PCR system (Life Technologies), using the manufacturers standard temperature profile. Using qBasePLUS software (v3.1), the delta-delta-Cq model was used to determine relative target gene expression.

2.7. Data processing

Raw sequencing reads were quality assessed with FastQC (Babraham Institute, Cambridge, UK). To pass the initial QC check, the average Phred score of each base position across all reads had to be at least 30. Reads were further processed by cutting individual low-quality bases and removing adapter and other Illumina-specific sequences with Trimmomatic V0.32 using default parameters (Bolger, 2014). Since the trimming process may result in some reads being discarded and their mates thereby unpaired, only reads that remained paired after trimming were used for downstream analyses. HISAT2 (Kim, 2015) was then used to first build a transcriptome index based on ENSEMBL annotations and then to map the trimmed reads to the human GRCh38

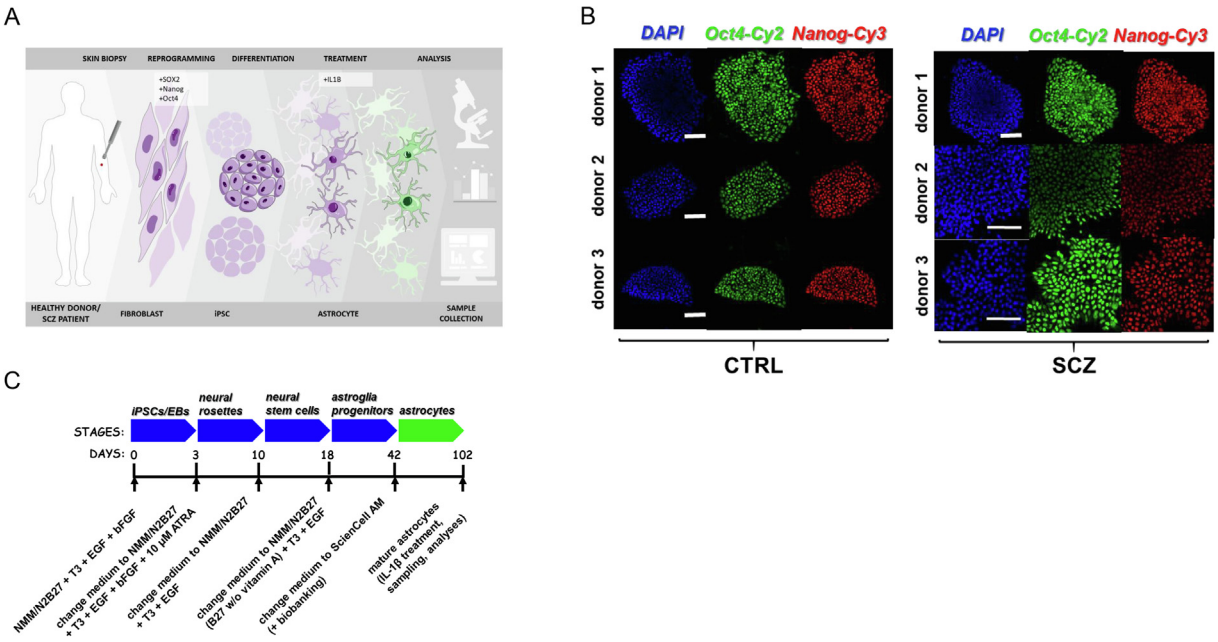

Fig. 1. iPSC derivation and characterization. (A) Diagram of the main stages of the study. This figure was created using Servier Medical Art templates, which are licensed under a Creative Commons Attribution 3.0 Unported License; https://smart.servier.com (B) Representative confocal microscopy images of iPSC lines (at passage 15) derived from 3 SCZ patients and 3 CTRLs. Cells are staining positive for Oct4 and Nanog pluripotency markers. Scale bar: 100 µm. (C) An overview of the applied protocol for astrocyte differentiation, activation, and analysis. For details, see Materials and Methods.

reference transcriptome. To quantify gene expression levels, mapped reads were summarized at the gene level using featureCounts (Liao, 2014) guided by ENSEMBL annotations.

2.8. Differential expression analysis

Before conducting the differential expression (DE) analyses, genes with very low to zero expression were removed by filtering out any gene with < 1 read count per million (CPM) in more than 3 samples (the smallest group sample size). DE analysis was performed using the statistical R package *DESeq2*, which provides methods to test for differentially expressed genes by use of negative binomial generalized models (Love, 2014). We performed 3 different DE analyses to examine the following: a) how cytokine treatment affects gene expression in CTRL subjects, b) how cytokine treatment affects gene expression in SCZ patients, and c) whether the effects of cytokine treatment on gene expression are different across SCZ and CTRL groups. Donor-specific variations were controlled for in all three experiments. In addition, to take into account that individuals were nested within diagnostic groups in the third analysis, the design formula was modified in accordance with the recommendations provided in the *DESeq2* vignette. The *DESeq2* workflow begins by taking raw read count data as input and applies an internal normalization method that corrects for sequencing depth and RNA composition. After the standard DE analysis which consists of size factor estimation, dispersion estimation, and model fitting, *DESeq2* performs an independent filtering step that optimizes the number of genes with adjusted p-values below a user-specified significance level (0.05 in the present study) (Love, 2014). After the pre-filtering and independent filtering steps, a total of 17,880 genes were examined in the 3 DE analyses.

2.9. Pathway enrichment analysis

Pathway analysis of the nominally significant DE genes identified in the third analysis was performed separately for the relatively up and down-regulated genes using *pathfindR* with default parameters (Ulgen, 2018). Rather than treating all genes equally as many pathway analysis tools do, *pathfindR* takes into account both the p-values and effect sizes of individual genes. It also incorporates information on protein–protein interactions between genes and thereby avoids the assumption that each gene is independent from the other genes. The Kyoto Encyclopedia of Genes and Genomes (KEGG) database (Kanehisa and Goto, 2000) was used as the pathway reference database, except that we excluded all pathway terms related to human diseases since we were primarily interested in the molecular mechanisms and biological processes that the identified DE genes are involved in.

2.10. Immunocytochemistry (ICC) and imaging

Samples were fixed with 4% paraformaldehyde for 10 min, and washed 3 times with PBS for 15 min. Samples were blocked for 1 h with 10% normal horse serum (NHS; Abcam) in Tris-buffered saline containing 0.5% (v/v) Triton X-100, pH 7.4 (TBSTx). Fixed cells were further incubated overnight in 1% NHS in TBSTx with rabbit anti-GFAP (diluted 1:500; Dako-Agilent) or goat anti-GFAP (diluted 1:500), rabbit anti-S100B (1:400), rabbit anti-AQP4 (1:500), rabbit anti-MAP2 (diluted 1:400), mouse anti-NG2 (diluted 1:500), mouse anti-Oct4 or rabbit anti-Nanog antibodies (all from Abcam). Samples were then rinsed 3x with 1% NHS in TBSTx and and blocked again for one hour at RT. Samples were incubated with secondary antibodies (1:500) for 2 h at RT: Alexa Fluor 488 donkey anti-mouse IgG, Alexa Fluor 555 goat anti-rabbit IgG, Alexa Fluor 647 donkey anti-goat IgG, Cy3 anti-rabbit IgG, Cy2 anti-mouse (all from Abcam). The samples were then rinsed 3x with 1% NHS in TBSTx and incubated for 5 min with the nuclear stain Hoechst 33258 or DAPI (1 µg/ml in PBS; Sigma). The samples were then rinsed for 10 min in PBS and mounted under coverslips in PBS:glycerol 1:1. The samples were examined and imaged with a Zeiss LSM 700 confocal microscope, or an Olympus AX70 fluorescent microscope. Images were processed using ImageJ software version 1.52p (National Institutes of Health, USA). The number of GFAP-positive astrocytes was obtained by automated cell counting using an ImageJ macro as previously described (Boulland, 2012).

2.11. ELISA assays

For sample preparation, 2.5 × 10^5 cells were cultured in 1 ml AM medium in 12-well plate. Culture supernatants were harvested 24 h after activation by 10 ng/ml IL-1β and the concentration of CCL20 chemokine was measured using MIP-3 alpha/CCL20 Human ELISA kit (Thermo Fisher) following the manufacturer's recommendations. For HILPDA protein level measurements samples were prepared by lysing 2.5 × 10^5 cells following 24 h IL-1β treatment. Lysis of iPSC-astrocytes was done using Pierce IP Lysis Buffer (Thermo Fisher) following the recommended protocol. The protein level of HILPDA was assessed using a human HILPDA/HIG2 ELISA kit (LSBio, Seattle, WA, USA). The precision of the ELISA kits were the following: Intra-Assay variation: CV < 10%; Inter-Assay variation: CV < 12% (CV% = SD/meanX100).

2.12. Isolation and phenotyping of regulatory T lymphocytes

Leukocyte-enriched buffy coats were obtained from anonymous healthy blood donors drawn at the Oslo University Hospital Blood Bank in accordance with the institutional guidelines. All enlisted donors were healthy persons residing in Norway during the study period. Written informed consent was obtained from the donors prior to blood donation, and their data were processed and stored according to the directives of the Norwegian Scientific Ethical Committees and the Norwegian Data Protection Agency. Peripheral blood mononuclear cells (PBMCs) were separated by a standard density gradient centrifugation with Ficoll-Paque Plus (Amersham Biosciences, Uppsala, Sweden). T_{regs} were isolated from PBMC by CD4-negative selection followed by CD25-positive selection, using a $CD4^+CD25^+$ T cell isolation kit (Miltenyi). After separation on a VarioMACS magnet, 95–98% of the cells were $CD4^+CD25^+$ T cells as measured by flow cytometry (Supplementary Table 1). Phenotyping of T_{regs} was performed by flow cytometry using anti-CD4-FITC, anti-CD25-PE, and anti-CCR6-FITC (Abcam), and isotype-matched control antibodies (BD Pharmingen, San Jose, CA, USA). Fluorescence intensities were measured by FACS Calibur (BD Biosciences, Franklin Lakes, NJ), data were analyzed by the FlowJo software (Tree Star, Ashland, OR).

2.13. In vitro transwell chemotaxis assay

The chemotaxis protocol was performed as described previously (Zhang, 2009). Briefly, after isolation, $CD4^+CD25^+$ T cells were incubated at 5% CO_2 at 37C for 24 h before performing the chemotaxis assay. Specific regulatory T cell migration was assessed by an 5 μm Transwell system (Corning, Lowell, MA). A total of 5 × 10^5 CFSE labeled $CD4^+CD25^+$ T_{reg} cells in RPMI 1640 containing 0.5% fatty acid-free BSA (Sigma) were added in a volume of 100 μl to the upper wells of a 24-well transwell plate with an 5 μm insert (Corning International, Corning, NY, USA). 600 μl of AM medium (spontaneous migration ctrl), or non-diluted supernatants from astrocyte cultures (24 h 10 ng/ml IL-1β treated or non-treated, CTRL or SCZ) were added to the lower compartment. The number of T lymphocytes that migrated to the lower well following a 4-hour incubation step were counted under a fluorescent microscope using a hemocytometer.

2.14. CCR6 receptor neutralization

To block CCR6 receptor on $CD4^+CD25^+$ T lymphocytes, isolated cells were treated with 10 μg/ml of anti-CCR6 polyclonal antibody (extracellular domain-specific, Abgent, San Diego, CA, USA) or an IgG isotype-matched control antibody (Biolegend, San Diego, CA, USA) for 1 h prior to migration assay set-up. Before assaying, cells were washed two times using warm, sterile, serum-free RPMI medium and centrifuged at 300 rpmi for 5 min to remove excess antibodies.

2.15. Glutamate uptake assay

Indirect assessment of glutamate uptake by resting iPSC-astrocytes was done using a colorimetric glutamate assay kit following the manufacturer's recommendations (Abcam; Cat. no.: ab83389). Briefly, cells were incubated in AM medium at 37 °C and 5% CO_2 for 24 h then supernatants were collected and assayed. Native AM cell medium (medium control) and donor/clone-specific iPSC lines were used as controls.

2.16. Statistics

In vitro T cell migration results represent mean values of triplicate samples from SCZ and CTRL culture supernatants. All experiments were performed three times using T cells from 3 independent healthy donors. Data are presented as mean ± standard deviation. Comparisons between groups were done by independent sample t-tests or analysis of variance (ANOVA) between groups. To test for significant differences in the blood gene expression levels of T_{reg} markers (*CCR6* and *FOXP3*) in SCZ patients compared to CTRLs, a multiple linear regression model with adjustment for age and sex differences was performed in R 3.4.1.

3. Results

3.1. Generation and characterization of iPSC-astrocytes from SCZ and CTRL subjects

3.1.1. Generation of iPSC-astroglia

To establish an *in vitro* human cellular model for evaluating the effects of inflammatory modulation on iPSC-astroglia, we first reprogrammed fibroblasts isolated from SCZ (n = 3) and CTRL donors (n = 3) using Sendai virus vector (Fig. 1A; see Table 1 for a summary of donor characteristics, and Materials and Methods for details on their origin and derivation). On average, 3–5 clones were generated per donor iPSC lines and were cultured for at least 5–10 passages to allow time for the wash-out of virus before pluripotency testing. At passage 15, both control and patient iPSC lines stained positive for the pluripotency markers Oct4 and Nanog (Fig. 1B), and robustly expressed the *Oct4*, *Nanog*, and *Sox2* genes (Fig. S1). One clone per donor was selected for experiments and cultured for an additional 9–10 passages including massive-scale cell banking in liquid nitrogen. Each *in vitro* experiment was done in triplicates if not stated otherwise.

At passage 24–25 of the selected iPSCs, we derived astrocyte-like cells using slightly modified versions of two previously published glial differentiation protocols (Fig. 1C) (Izrael, 2007; Tcw, 2017). The applied retinoic acid (ATRA)-based neural induction conditions successfully generated cell populations with rosette-like structures derived from embryiod bodies (EBs). Areas outside the neural rosettes exhibited varying morphologies. To evaluate the different neural progenitor (NP) populations for the expression of known markers and monitor the differentiation of astrocytes from the earliest stages (day 0/iPSC), a custom-made TLDA gene array was used to measure the expression of the NP markers PAX6 (transcription factor regulating gene expression during nervous system development) and Nestin (a type VI intermediate filament protein expressed in multiplying cells of the developing nervous system), as well as of the key astrocyte markers GFAP (Glial fibrillary acidic protein), S100B (S100 calcium-binding protein B), AQP4 (Aquaporin 4), SLC1A2 and SLC1A3 (Solute Carrier Family 1 Member 2 and 3), and additional astroglia-specific markers: FABP7 (Fatty acid binding protein 7), ALDH1L1 (Aldehyde Dehydrogenase 1 Family Member L1), and ALDOC (Aldolase C).

3.1.2. Characterization of iPSC-astroglia

In general, all cultures in the neural rosette/NP stage highly expressed the critical markers PAX6 and NES, and these markers were continuously expressed, although gradually downregulated throughout

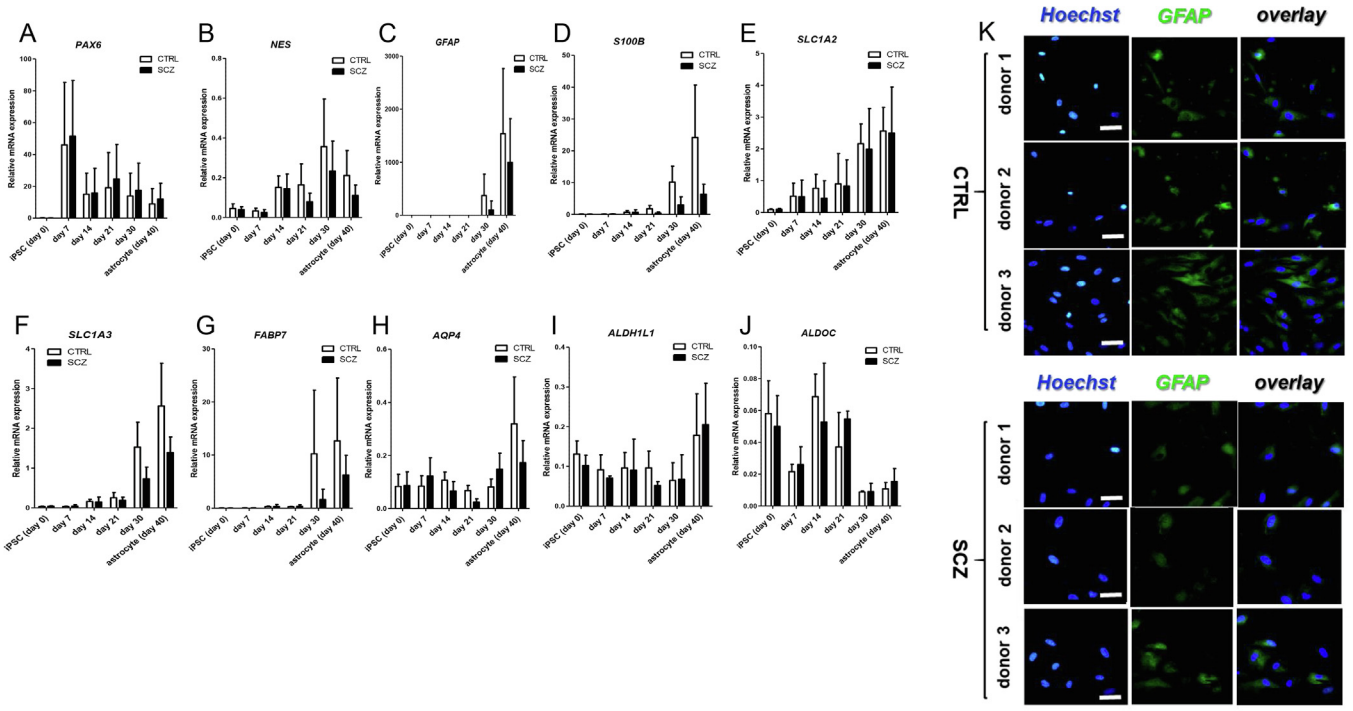

Fig. 2. iPSC-derived astrocyte differentiation and characterization. (A–J) Gene expression analysis of neural stem cell (*PAX6, NES*) and astrocyte-specific markers (*GFAP, S100B, SLC1A2, SLC1A3, FABP7, AQP4, ALDH1L1, ALDOC*) in SCZ (black bars) and CTRL cultures (empty bars). Samples were collected during differentiation from day 0 (iPSC) until day 40 and were analyzed using a custom-made TLDA gene array card (qPCR). Data of triplicate measurements of three independent donors per group are presented as Mean ± SEM. K) Representative immunocytochemistry images of day 42 ("early") astrocytes derived from 3 SCZ patients and 3 CTRLs. Cells are stained positive for the specific astroglial marker GFAP. Scale bar: 150 μm.

the differentiation process, in early astrocyte progenitors and fully differentiated astrocytes (Fig. 2A and B), in agreement with the literature (Krejciova, 2017; Ho, 2017; Nadadhur, 2018). Astrocyte cultures were successfully established from iPSC lines of both SCZ patients and CTRLs. All lines exhibited the typical expression kinetics of developing astroglia marker genes (*GFAP*; *S100B*, *AQP4*, *SLC1A2*, *SLC1A3*, *FABP7*, and *ALDH1L1* - Fig. 2C–I) (Molofsky and Deneen, 2015). Astroglial markers that appear later in development (including GFAP, S100B, SLC1A2, SLC1A3, and FABP7) showed robust mRNA expression only in later stages (day 30 and 40 samples, Fig. 2C–G) corroborating a successful differentiation trajectory of cell cultures (Molofsky and Deneen, 2015; Krencik, 2017). On day 40, *AQP4* and *ALDH1L1* gene expressions increased only modestly (Fig. 2H and I), while *ALDOC* mRNA expression was not modulated significantly throughout the differentiation process until this point (Fig. 2J) suggesting a skewing process towards protoplasmic astroglial cellular identity in early iPSC-astrocytes (Cahoy, 2008; Morel, 2017). No statistically significant differences were observed between patients and controls in the gene expression pattern of the astrocyte-specific markers at any time point up until day 40 (Fig. 2A–J). The astroglial phenotype of iPSC-derived cells was further confirmed by ICC detection demonstrating expression of the key astrocyte marker GFAP in all iPSC-derived astrocyte cultures on day 42 (Fig. 2K).

After day 42, "young" astrocytes were cultured further for an additional 60 days (~15–20 passages) in ScienCell AM medium that has been previously shown to strongly promote and maintain iPSC-astroglial differentiation and maturation, as well as select for astrocytes in *in vitro* cultures (Tcw, 2017). Our ICC results showed massive enrichment (~99% purity) of astroglia, and robust expression of the astrocyte-specific markers GFAP, S100B, and AQP4 in all iPSC-astrocyte cultures on day 102 (Fig. 3A). Furthermore, no evident contamination by other cell types, such as neurons or oligodendroglial progenitors could be seen as tested by immunostaining with anti-MAP2 or anti-NG2 antibodies, respectively (Supplementary Fig. S2). "Mature" astrocyte phenotype was further confirmed by qPCR results showing the maintained gene expression of *GFAP* and *FABP7* markers, and a strong increase in the mRNA levels of *S100B*, *ALDH1L1*, *AQP4*, and *SLC1A2* compared to "young" (day 42) astrocytes (Fig. 3B–G). We demonstrated the functionality of mature astroglia by using a specific glutamate uptake assay showing that CTRL and SCZ astroglia are capable of the uptake process, but that non-astrocytic (iPSC) controls are not (Fig. 3H). Both CTRL and SCZ iPSC-astrocytes demonstrated effective uptake of glutamate relative to control (iPSC) cell cultures, and medium control. No significant difference was observed between CTRL and SCZ iPSC-astroglia in glutamate uptake (Fig. 3H).

3.2. Inflammatory modulation and comparative analysis of SCZ and CTRL-derived iPSC-astrocytes

We next tested the effects of cytokine treatment on iPSC-astrocytes. To mimic inflammasome activation, we applied physiologically relevant concentrations (0.1, 1, and 10 ng/ml) (Woiciechowsky, 1999; Cacabelos, 1994) of IL-1β and investigated the short-term (4 h) effect on early-response inflammatory cytokine genes using qPCR (Medzhitov, 2001). All applied concentrations of IL-1β strongly increased the expression of *CXCL8/IL-8*; *IL6*, and *TNF* genes in both SCZ and CTRL iPSC-astrocytes, with no differences between patient and control lines (Fig. S3). In general, the most pronounced effect was seen at an IL-1β concentration of 10 ng/ml (Fig. S3), and this concentration was therefore used in subsequent experiments.

3.2.1. Unsupervised clustering

Principal Component Analysis (PCA) was used to cluster astrocyte samples based on all expressed genes. We found a clear separation on donor when clustering over the first two principal components (PCs), explaining 64% of the variation in total (Fig. 4A). When clustering over PC3 and PC4, we found a good separation on condition (IL-1β treated vs. untreated) and diagnostic status (CTRL vs. SCZ), explaining 21% of

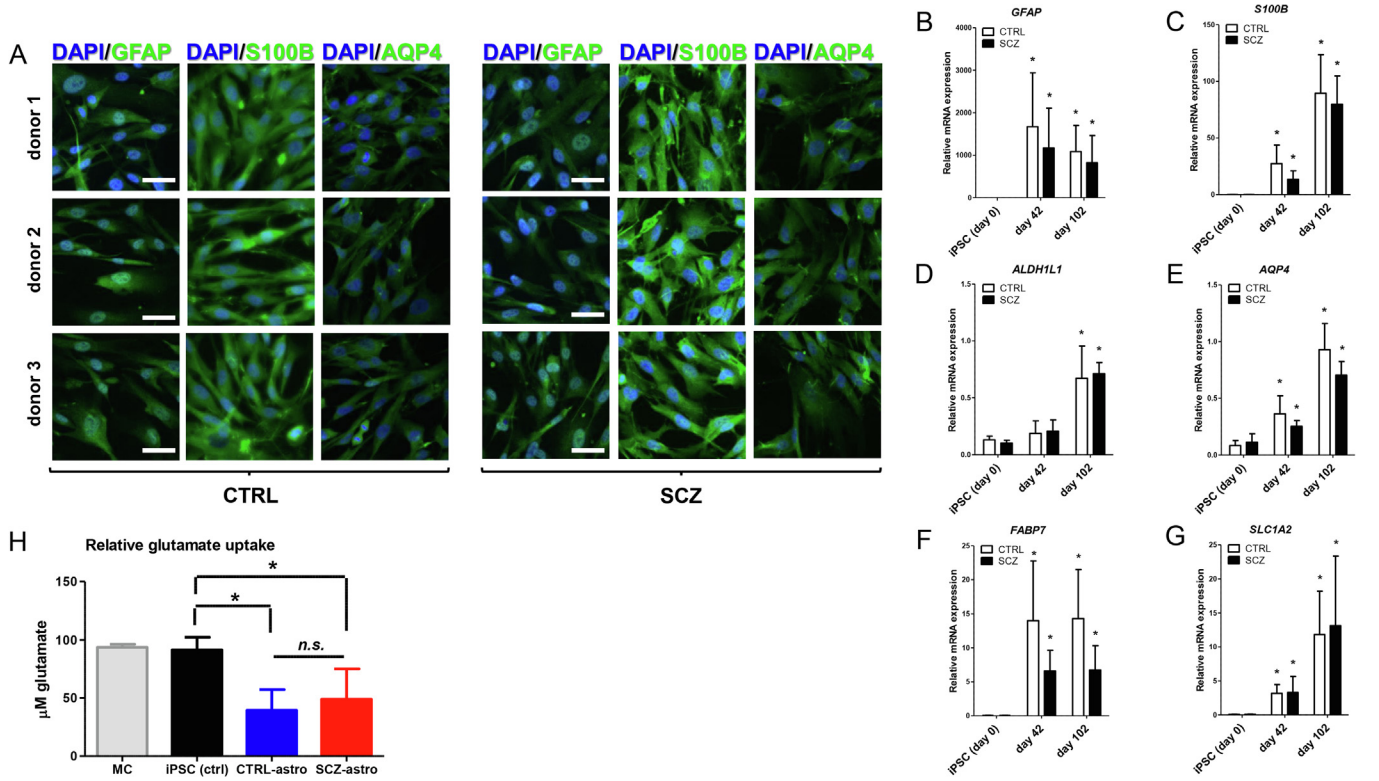

Fig. 3. Characterization of mature iPSC-derived astrocytes. (A) Cells from day 102 cultures stained positive for the key astrocyte markers GFAP, S100B, and AQP4. Representative images from 3 donors with SCZ and 3 CTRLs are presented. Scale bar: 200 µm. (B-G) Gene expression screening of astroglia-specific markers in SCZ (black bars) and healthy mature CTRL astrocyte cultures (empty bars). Samples were collected at days 0 (iPSC), 42 (early astrocyte), and 102 (mature astrocyte) and analyzed using qPCR. Data of triplicate measurements of three independent donors per group are presented as Mean ± SEM. Asterisks represent statistically significant differences between day 42/102 cells and day 0 (iPSC) cells at $p < 0.05$. (H) Glutamate uptake of resting iPSC-astrocytes was assessed using a glutamate assay kit. Native AM cell medium (MC – "medium control"), and donor/clone-specific iPSC lines were used as controls (iPSC ctrl). Data of triplicate measurements of three independent donors per group are presented as Mean ± SEM (in the case of MC, triplicate measurements were performed by sampling the same bottle of medium in which all cells were cultured). Asterisks represent significant differences relative to iPSC controls at p values < 0.05; *n.s.* = "non-significant".

the variation in total (Fig. 4B). These results suggest that the donor effect is an important source of gene expression variation that must be accounted for when identifying the effects that are due to cytokine treatment and diagnosis.

3.2.2. Differential expression analyses in CTRL and SCZ groups

We first performed two separate DE analyses investigating the gene expression effects of IL-1β exposure in CTRL and SCZ samples, respectively. In the CTRL group, the treatment significantly changed the gene expression levels of 2213 genes (12.4%). Of these, 1358 genes (61.4%) were up-regulated and 855 genes (38.6%) were down-regulated (Fig. 4C; Supplementary Table S2). In the SCZ group, IL-1β modulated the expression of only 779 genes (4.4%): 599 (76.9%) up-regulated and 180 (23.1%) down-regulated (Fig. 4D; Supplementary Table S3). The DE genes in both CTRL and SCZ groups had a similar dynamic range of effect sizes (log2FCs from −2 to −10), and 647 genes were shared by both groups (Fig. 4E). Moreover, the effect sizes of the shared genes were highly correlated ($r = 0.96$; Fig. 4F). Most of the genes affected by IL-1β stimulation were protein-coding (> 85%), but also some miRNA and long non-coding RNAs were modulated (Supplementary Tables S2-3). In general, genes involved in immunological functions were among the most affected, such as *TNF*, *CXCL11*, and *IL1B* (Supplementary Tables S2-3).

3.2.3. Group-specific gene expression effects of cytokine treatment

To examine whether SCZ iPSC-astrocytes responded differently to IL-1β exposure than CTRL astrocytes, we performed a group-specific differential expression analysis. We found that 458 genes were modulated differently across groups at the nominal significance level of $p < 0.05$ (Fig. 5A, Supplementary Table 4). Of these genes, 255 were relatively up-regulated, i.e. either more up-regulated or less down-regulated in the SCZ group compared to the CTRL group, while 203 genes were relatively down-regulated, i.e. either less up-regulated or more down-regulated in SCZ than in CTRL. Two genes remained statistically significant after multiple testing correction: *CCL20* ($p = 5.54e\text{-}6$, $logFC = -1.58$) and *HILPDA* ($p = 5.01e\text{-}6$, $logFC = -1.06$). For both of these genes, the up-regulatory effect of IL-1β treatment was smaller in SCZ than in CTRL subjects (Fig. 5B). Separate pathway analyses of the relatively up and down-regulated DE genes suggested an enrichment for genes involved in cell cycle, signal transduction, apoptotic, and neuronal processes (Fig. 5C, Supplementary Table 5).

3.3. Reduced CCL20 secretion by SCZ astrocytes underlies decreased migration of human T_{reg} cells

Next, we sought to validate the *HILPDA* and *CCL20* RNA-Seq results using qPCR and ELISA assays. The qPCR analysis showed that IL-1β treatment enhanced *HILPDA* and *CCL20* mRNA expressions in CTRL iPSC-astrocytes compared to SCZ cells, confirming the different stimulatory effect of IL-1β on the expression levels of these two genes as revealed by RNA-Seq (Fig. 6A–C). Consistent with these results, SCZ astrocytes secreted a significantly lower amount of the CCL20 cytokine than CTRL iPSC-astroglia when culture supernatants were tested using ELISA (Fig. 6D). Furthermore, we could not detect HILPDA protein in iPSC-astrocytes neither at baseline nor after IL-1β treatment (high-sensitivity ELISA, data not shown). To test the functional consequences of reduced CCL20 secretion, we next investigated if IL-1β-activated

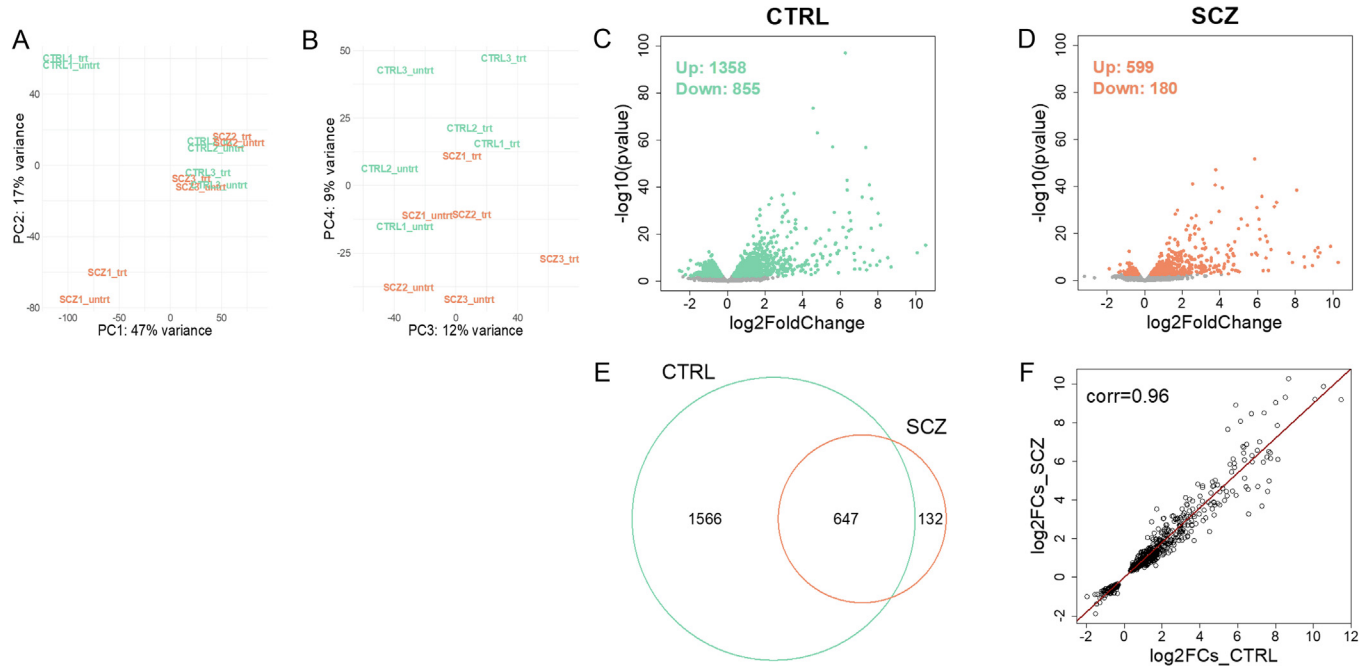

Fig. 4. Effects of cytokine stimulation on global gene expression levels in iPSC-derived SCZ and CTRL astrocytes. A) PCA plot showing good separation on donor across the first two PCs. B) When clustering across PC3 and PC4, a clear separation on treatment and diagnosis appears, explaining 21% of the gene expression variance. C) The effect of cytokine treatment on gene expression in CTRL astrocytes. 1358 genes were significantly up-regulated and 855 were down-regulated, with effect sizes ranging from log2FC −2 to 10. D) The effect of cytokine treatment on gene expression in SCZ astrocytes. 599 genes were significantly up-regulated and 180 were down-regulated. E) Overlap of significantly expressed genes in CTRL and SCZ astrocytes. F) Scatter plot showing the correlation of log2FCs for the 647 overlapping genes significantly regulated by cytokine treatment in both CTRL and SCZ samples. These genes were highly correlated in terms of both the direction and magnitude of effect sizes. PC: Principal component, FC: Fold change.

astrocytes were capable of stimulating the migration of human $CD4^+CD25^+$ T_{reg} cells known to express the CCL20 chemoattractant-specific chemokine receptor 6 (CCR6) (Kleinewietfeld, 2005). Our migration assay results showed that IL-1β-stimulated SCZ astrocytes triggered a weaker migratory response compared to CTRL cells by attracting significantly lower number of T_{reg} cells in the assay setup (Fig. 6E). Remarkably, this disparate chemoattracting effect on cell migration between CTRL and SCZ was completely abrogated by blocking the CCR6 receptor of T_{regs}, demonstrating the critical importance of the CCR6-CCL20 axis in the observed phenomenon (Fig. 6E).

3.4. Decreased expression of the T_{reg} specific transcription factor FOXP3 in SCZ patients

Since our findings suggested a possible link between defective astrocyte functions and regulatory T cell migration dynamics in SCZ, we next investigated whether the two T_{reg}-specific markers, *CCR6* and *FOXP3*, were differentially expressed in whole-blood samples from a large cohort of SCZ patients (n = 484) and CTRLs (n = 472) (Fig. 7). We found that SCZ patients had a slightly lower expression of *FOXP3* that was statistically significant after controlling for age and sex (p = 0.0137). No significant difference between patients and controls was seen for *CCR6* (Fig. 7). These results suggest a possible disease-specific T_{reg} cell defect in SCZ.

4. Discussion

In the present study, we explored the global transcriptomic effects of IL-1β modulation on human iPSC-derived astrocytes generated from SCZ and CTRL participants. We successfully established an *in vitro* iPSC-astroglia model and found that inflammasome activation, as mimicked by short-term IL-1β treatment, had a reduced up-regulatory effect on *CCL20* and *HILPDA* expression in SCZ. The effect on CCL20 was also confirmed at protein levels, and importantly, IL-1β activated iPSC-derived astrocytes had a weaker chemotactic effect on T_{reg} cells. Our blocking experiments suggested that this effect was mediated by astrocyte-derived CCL20. Based on the ability of T_{reg} cells to control inflammation, our findings may suggest the attenuated CCL20 response may contribute to a dysregulated brain inflammation in SCZ.

Understanding the mechanisms by which the immune system and cytokines contribute to neuropsychiatric diseases could lead to the identification of novel drug targets. According to recent findings, such targets involve several inflammatory pathways including MAPKs, Nf-kappaB, indoleamine-2,3-dioxygenase, and many others (Haroon, 2012). Previous studies have also showed altered expression of several chemokines which again may influence the recruitment of various lymphocyte subsets such as inflammatory T_h1 and T_h17 and anti-inflammatory T_{reg} cells to the affected brain regions (McGlasson et al., 2015). Brain inflammation due to dysregulated microglia functions and inflammasome activation has been hypothesized to play an important role in SCZ pathophysiology (Khandaker, 2015; Kim, 2016). Moreover, IL-1β gene expression levels and polymorphism have also been associated with SCZ symptom severity (Hänninen, 2008; Ghafelehbashi, 2017).

HILPDA (hypoxia-inducible lipid droplet-associated, also known as HIG2) is an adipocyte-associated factor involved in lipid droplet formation and metabolism, but also in IL-6 inflammatory *trans*-signaling (Robinson, 2015; Jiang, 2015). Its biological function is not known yet, but its expression is subject to strict translational/post-translational control in many cell types, such as bone marrow-derived mesenchymal stem cells, and the functional HILPDA protein is expressed only under hypoxic stress (Jiang, 2015). Consistent with this, we found no detectable levels of HILPDA protein in iPSC-astrocytes neither at baseline nor after inflammatory stimulation, and the potential role of HILPDA in SCZ should be further investigated using hypoxic experimental conditions.

CCL20 is a chemokine that can be released by various cell types

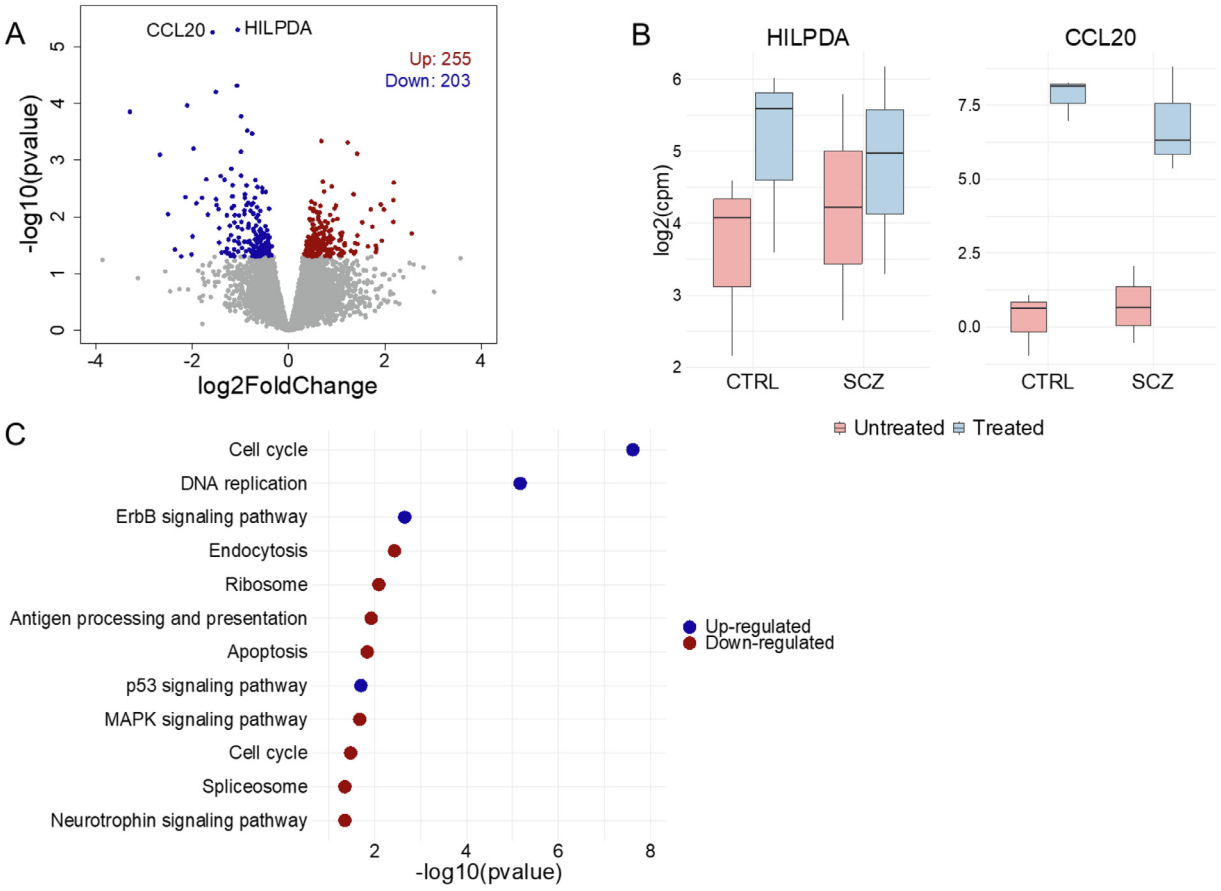

Fig. 5. Group-specific effects of cytokine treatment on global gene expression levels. A) Volcano plot showing cytokine-induced up and down-regulated genes in SCZ astrocytes relative to CTRL astrocytes. With the exception of *CCL20* and *HILPDA*, these genes were nominally significant at $p < 0.05$. B) Cytokine treatment resulted in a reduced up-regulation of *HILPDA* and *CCL20* in SCZ relative to CTRL. The effect remained significant after adjusting for multiple testing. C) Pathway analysis of the nominally significant genes (including *HILPDA* and *CCL20*). Up-regulated genes showed strongest enrichment for molecular pathways related to cell cycle and DNA replication, while down-regulated genes showed strongest enrichment for pathways involved in endocytosis and ribosome-related processes. CPM: Counts per million.

including astrocytes (Rothhammer and Quintana, 2015) and peripheral blood mononuclear cells during inflammation, and is a highly specific ligand for the non-promiscuous chemokine receptor CCR6 (Schutyser, 2003). The extreme selectivity of the CCR6/CCL20 ligand-receptor interaction, in contrast to the binding characteristics of other chemokine receptors, suggests a tightly regulated function (Schutyser, 2003). The expression of CCR6 is restricted to only a few immune cell types including a subset of IL-10 producing anti-inflammatory T_{regs} with high migratory capacity towards tissue CCL20 signals (Kleinewietfeld, 2005; Rivino, 2010; Cook, 2014; Liu, 2015). The physiological importance of the CCL20-CCR6-T_{reg} axis in regulating inflammatory processes in many tissues has been noted by others (Kleinewietfeld, 2005; Rivino, 2010). Our results showed that IL-1β-treated SCZ iPSC-astrocytes secreted significantly lower amounts of CCL20 than CTRL cells, and the functional consequence of this phenomenon was also demonstrated using a T cell migration assay where SCZ astrocytes induced the migration of T_{regs} to a much lower degree than CTRL iPSC-astrocytes in a CCL20-CCR6-dependent manner. Besides their role in regulating the general neurophysiology of the brain, astrocytes also contribute to neuroimmune homeostasis. Our finding thereby suggest that the CCL20-mediated regulation of T_{reg} chemotaxis, potentially also from the blood to the brain, could be an important feature of astrocyte-mediated immune regulation (Trajkovic, 2004; Ito, 2019). Dysregulated inflammasome activation and the consequent release of IL-1β into the brain parenchyma have been linked to a wide spectrum of neuropsychiatric pathologies ranging from neurodegeneration (Heneka, 2018) to SCZ (Khandaker, 2015). Based on our results, we hypothesize that a defective astroglia-CCL20-CCR6-T_{reg} axis may represent a biological component of SCZ. We propose that a decreased number of anti-inflammatory T_{regs} in the periphery and/or their reduced ingress to the brain, due to the impaired ability of astrocytes to produce inflammation-modulating CCL20 molecules, fails to properly regulate CNS inflammation potentially contributing to the "inflammatory arm" in the pathogenesis of of SCZ. This hypothesis is supported by recent clinical findings showing increased numbers of circulating T_{regs} in SCZ patients compared to the non-medicated SCZ group (Kelly, 2018). Further support for this hypothesis can be found in our results showing lower expression of the T_{reg}-specific transcription factor *FOXP3* in the whole blood of SCZ patients relative to CTRLs, suggesting decreased number/activity of T_{regs} in patients.

The field of psychiatry needs cellular and molecular biomarkers to successfully address questions regarding the pathophysiological basis of different mental disorders. Here we established a human *in vitro* iPSC-based cellular model that presents astroglial features and phenotypes both during differentiation and maturation. This model displays functional immunocompetence by responding to IL-1β treatment via the upregulation of early inflammatory response cytokine and chemokine genes, as well as by secreting high levels of the $CCR6^+$ T_{reg}-attracting chemokine CCL20. We identified defective IL-1β-induced CCL20 responses in SCZ astrocytes compared to controls resulting in impaired chemotactic activity on T_{regs} as a major feature of iPSC-astrocytes in SCZ patients. Our results support the "immunopsychiatric" or "gliopathy" hypothesis of SCZ, pointing to the possible involvement of astrocytes in the process. We propose that the astroglia-CCL20-CCR6-T_{reg}

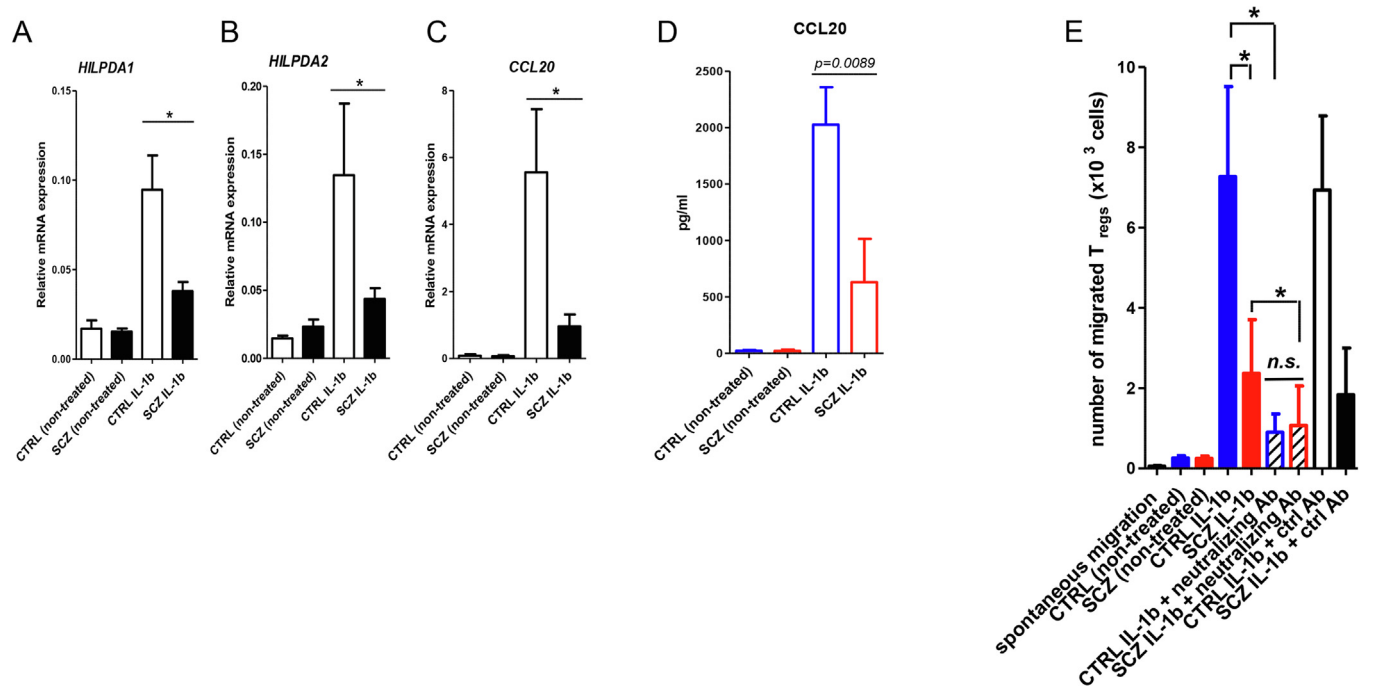

Fig. 6. Effects of IL-1β treatment in iPSC-derived astrocytes. (A-C) qPCR validation of *HILPDA* and *CCL20* RNA-Seq expression data in SCZ astrocytes (black bars) and healthy controls (empty bars) following IL-1β treatment. For HILPDA mRNA expression measurements both available Taq-Man probes (targeting two, partially overlapping isoforms) were used (Fig. 6A and 6B). Data of triplicate measurements of three independent donors per group are presented as Mean ± SEM. Asterisk means p values < 0.05. (D) Assessing CCL20 cytokine secretion in IL-1β-activated astrocyte cultures using ELISA. Mature astrocytes from 3 patients with SCZ (red bars) or 3 CTRLs (blue bars) were treated with 10 ng/ml IL-1β for 24 h and supernatants were collected for cytokine measurements. Data of duplicate measurements of three independent donors per group are presented as Mean ± SEM. (E) Effect of 10 ng/ml IL-1β-treated astrocyte culture supernatants on the migration of human T_{reg} cells. Migration assay was performed as described in Materials and Methods. Striped bars mean CTRL (blue) or SCZ (red) astrocyte supernatants modulating the migration of T_{regs} following CCR6 receptor neutralization. White (CTRL) and black bars (SCZ) represent isotype control Ab setups. Data of duplicate measurements of three independent donors in each group using pooled migration data of T_{reg} cells isolated from 3 healthy donors are shown as Mean ± SD. Asterisk represents p values < 0.05. (*n.s.* = "non-significant"). (For interpretation of the references to colour in this figure legend, the reader is referred to the web version of this article.)

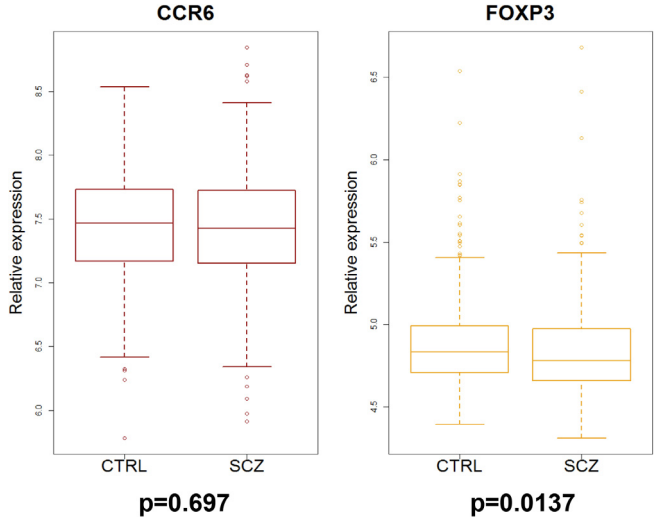

Fig. 7. Expression of T_{reg}-specific marker genes in whole blood of SCZ patients and CTRL subjects. *FOXP3* was slightly but significantly down-regulated in SCZ patients compared to CTRL ($p = 0.0137$, $\beta = -0.044$). No significant difference in gene expression level was found for *CCR6* ($p = 0.697$, $\beta = -0.010$).

axis emerges as a promising candidate in future pharmacological studies in SCZ, and potentially also in other neuropsychiatric disorders.

Acknowledgements

We thank all participants in this study for their invaluable contribution.

In addition the authors would like to thank Drs. Olav Smeland and Erlend Strand Gardsjord who were involved in patient recruitment and clinical assessments, research nurses Eivind Bakken and Line Gundersen for obtaining, organizing and processing skin biopsies samples, as well as research assistant Kristine Kjeldal for excellent technical asisstances with cultivation of fibroblasts and qPCRs. The authors also would like to thank Dr. Vivi Heine (VU University Medical Center Amsterdam) for her advices on the generation and characterization of iPSC-astrocytes. The authors are grateful for the professional assistance of Dr. Zsofia Foldvari (Oslo University Hospital) in creating the artwork of Fig. 1A.

We acknowledge the support and use of facilities at the Norwegian Core Facility for Human Pluripotent Stem Cells, under the Norwegian Center for Stem Cell Research. We thank in particular Prof. Joel Glover, Hege Brincker Fjerdingstad, and Kirstin Buchholz.

The sequencing service was provided by the Norwegian Sequencing Centre (www.sequencing.uio.no), a national technology platform hosted by the University of Oslo and supported by the Functional Genomics and Infrastructure programs of the Research Council of Norway and the Southeastern Regional Health Authorities.

The research leading to these results has received funding from the South-Eastern Norway Regional Health Authority (#2018094) and the Research Council of Norway (#223273).

Appendix A. Supplementary data

Supplementary data to this article can be found online at https://doi.org/10.1016/j.bbi.2020.02.008.

References

Akkouh, I.A., et al., 2018. Expression of TCN1 in blood is negatively associated with verbal declarative memory performance. Sci. Rep. 8, 12654.

Bechter, K., et al., 2010. Cerebrospinal fluid analysis in affective and schizophrenic spectrum disorders: identification of subgroups with immune responses and blood-CSF barrier dysfunction. J. Psychiatr. Res. 44, 321–330.

Benros, M.E., et al., 2011. Autoimmune diseases and severe infections as risk factors for schizophrenia: a 30-year population-based register study. Am. J. Psychiatry 168, 1303–1310.

Bolger, A.M., et al., 2014. Trimmomatic: a flexible trimmer for Illumina sequence data. Bioinformatics 30, 2114–2120.

Boulland, J.L., et al., 2012. Evaluation of intracellular labeling with micron-sized particles of iron oxide (MPIOs) as a general tool for in vitro and in vivo tracking of human stem and progenitor cells. Cell Transplant. 21, 1743–1759.

Brennand, K.J., et al., 2011. Modelling schizophrenia using human induced pluripotent stem cells. Nature 473, 221–225.

Cacabelos, R., et al., 1994. Brain interleukin-1 beta in Alzheimer's disease and vascular dementia. Methods Find. Exp. Clin. Pharmacol. 16, 141–151.

Cahoy, J.D., et al., 2008. A transcriptome database for astrocytes, neurons, and oligodendrocytes: a new resource for understanding brain development and function. J. Neurosci. 28, 264–278.

Cook, K.W., et al., 2014. CCL20/CCR6-mediated migration of regulatory T cells to the Helicobacter pylori-infected human gastric mucosa. Gut 63, 1550–1559.

Correll, C.U., et al., 2015. Effects of antipsychotics, antidepressants and mood stabilizers on risk for physical diseases in people with schizophrenia, depression and bipolar disorder. World Psychiatry 14, 119–136.

Corvin, A., Morris, D.W., 2014. Genome-wide association studies: findings at the major histocompatibility complex locus in psychosis. Biol. Psychiatry 75, 276–283.

DeLisi, L.E., et al., 2002. A genome-wide scan for linkage to chromosomal regions in 382 sibling pairs with schizophrenia or schizoaffective disorder. Am. J. Psychiatry 159, 803–812.

Dieset, I., et al., 2015. Association between altered brain morphology and elevated peripheral endothelial markers-implications for psychotic disorders. Schizophr. Res. 161, 222–228.

Editorial, 2010. A decade for psychiatric disorders. Nature 463, 9.

Falk, A., et al., 2016. Modeling psychiatric disorders: from genomic findings to cellular phenotypes. Mol. Psychiatry 21, 1167–1179.

Ghafelehbashi, H., et al., 2017. Decreased Expression of IFNG-AS1, IFNG and IL-1B Inflammatory Genes in Medicated Schizophrenia and Bipolar Patients. Scand. J. Immunol. 86, 479–485.

Hänninen, K., et al., 2008. Interleukin-1 beta gene polymorphism and its interactions with neuregulin-1 gene polymorphism are associated with schizophrenia. Eur. Arch. Psychiatry Clin. Neurosci. 258, 10–15.

Haroon, E., et al., 2012. Psychoneuroimmunology meets neuropsychopharmacology: translational implications of the impact of inflammation on behavior. Neuropsychopharmacology 37, 137–162.

Heneka, M.T., et al., 2018. Inflammasome signalling in brain function and neurodegenerative disease. Nat. Rev. Neurosci. 19, 610–621.

Ho, S.M., et al., 2017. Evaluating synthetic activation and repression of neuropsychiatric-related genes in hiPSC-derived NPCs, neurons, and astrocytes. Stem Cell Rep. 9, 615–628.

Hope, S., et al., 2013. Interleukin 1 receptor antagonist and soluble tumor necrosis factor receptor 1 are associated with general severity and psychotic symptoms in schizophrenia and bipolar disorder. Schizophr. Res. 145, 36–42.

International Schizophrenia Consortium, et al., 2009. Common polygenic variation contributes to risk of schizophrenia and bipolar disorder. Nature 460, 748–752.

Irish Schizophrenia Genomics Consortium and the Wellcome Trust Case Control Consortium 2, 2012. Genome-wide association study implicates HLA-C*01:02 as a risk factor at the major histocompatibility complex locus in schizophrenia. Biol. Psychiatry 72, 620–628.

Ito, M., et al., 2019. Brain regulatory T cells suppress astrogliosis and potentiate neurological recovery. Nature 565, 246–250.

Izrael, M., et al., 2007. Human oligodendrocytes derived from embryonic stem cells: Effect of noggin on phenotypic differentiation in vitro and on myelination in vivo. Mol. Cell. Neurosci. 34, 310–323.

Jiang, C., et al., 2015. HIF-1A and C/EBPs transcriptionally regulate adipogenic differentiation of bone marrow-derived MSCs in hypoxia. Stem Cell Res. Ther. 6, 21.

Kanehisa, M., Goto, S., 2000. KEGG: kyoto encyclopedia of genes and genomes. Nucleic Acids Res. 28, 27–30.

Kelly, D.L., et al., 2018. Increased circulating regulatory T cells in medicated people with schizophrenia. Psychiatry Res. 269, 517–523.

Khandaker, G.M., et al., 2015. Inflammation and immunity in schizophrenia: implications for pathophysiology and treatment. Lancet Psychiatry 2, 258–270.

Kim, D., et al., 2015. HISAT: a fast spliced aligner with low memory requirements. Nat. Meth. 12, 357–360.

Kim, H.K., et al., 2016. Nod-like receptor pyrin containing 3 (NLRP3) in the post-mortem frontal cortex from patients with bipolar disorder: A potential mediator between mitochondria and immune-activation. J. Psychiatr. Res. 72, 43–50.

Kim, R., et al., 2018. Astroglial correlates of neuropsychiatric disease: From astrocytopathy to astrogliosis. Prog. Neuro-Psychopharmacol. Biol. Psychiatry 87 (Pt A), 126–146.

Kindler, J., et al., 2019. Dysregulation of kynurenine metabolism is related to proinflammatory cytokines, attention, and prefrontal cortex volume in schizophrenia. Mol. Psychiatry. https://doi.org/10.1038/s41380-019-0401-9. [Epub ahead of print].

Kleinewietfeld, M., et al., 2005. CCR6 expression defines regulatory effector/memory-like cells within the CD25(+)CD4+ T-cell subset. Blood 105, 2877–2886.

Krejciova, Z., et al., 2017. Human stem cell-derived astrocytes replicate human prions in a PRNP genotype-dependent manner. J. Exp. Med. 214, 3481–3495.

Krencik, R., et al., 2017. (2017) Human astrocytes are distinct contributors to the complexity of synaptic function. Brain Res. Bull. 129, 66–73.

Liao, Y., et al., 2014. featureCounts: an efficient general purpose program for assigning sequence reads to genomic features. Bioinformatics 30, 923–930.

Liu, J.Y., et al., 2015. CTL- vs Treg lymphocyte-attracting chemokines, CCL4 and CCL20, are strong reciprocal predictive markers for survival of patients with oesophageal squamous cell carcinoma. Br. J. Cancer 113, 747–755.

Love, M.I., et al., 2014. Moderated estimation of fold change and dispersion for RNA-seq data with DESeq2. Genome Biol. 15, 550.

McGlasson, S., Jury, A., Jackson, A., Hunt, D., 2015. Type I interferon dysregulation and neurological disease. Nat Rev Neurol 11 (9), 515–523. https://doi.org/10.1038/nrneurol.2015.143.

Medzhitov, R., 2001. Toll-like receptors and innate immunity. Nat. Rev. Immunol. 1, 135–145.

Miyaoka, T., et al., 2017. Remission of psychosis in treatment-resistant schizophrenia following bone marrow transplantation: a case report. Front. Psychiatry 8, 174.

Mohammadi, A., et al., 2018. Brain, blood, cerebrospinal fluid, and serum biomarkers in schizophrenia. Psychiatry Res. 265, 25–38.

Molofsky, A.V., Deneen, B., 2015. Astrocyte development: a guide for the perplexed. Glia 63, 1320–1329.

Morch, R.H., et al., 2019. Inflammatory markers are altered in severe mental disorders independent of comorbid cardiometabolic disease risk factors - inflammatory markers and immune activation in severe mental disorders. Psychol. Med. https://doi.org/10.1017/S0033291718004142. [Epub ahead of print].

Morel, L., et al., 2017. Molecular and Functional Properties of Regional Astrocytes in the Adult Brain. J. Neurosci. 37, 8706–8717.

Nadadhur, A.G., et al., 2018. Patterning factors during neural progenitor induction determine regional identity and differentiation potential in vitro. Stem Cell Res. 32, 25–34.

Najjar, S., Pearlman, D.M., 2015. Neuroinflammation and white matter pathology in schizophrenia: systematic review. Schizophr. Res. 161, 102–112.

Rivino, L., et al., 2010. CCR6 is expressed on an IL-10-producing, autoreactive memory T cell population with context-dependent regulatory function. J. Exp. Med. 207, 565–577.

Robinson, M.B., et al., 2015. IL-6 trans-signaling increases expression of airways disease genes in airway smooth muscle. Am. J. Physiol. Lung Cell. Mol. Physiol. 309, L129–L138.

Rothhammer, V., Quintana, F.J., 2015. Control of autoimmune CNS inflammation by astrocytes. Semin Immunopathol 37, 625–638.

Rubinstein, E., 2010. Psychiatry: medicine benefits from cultural and personal insights. Nature 463, 424.

Schizophrenia Working Group of the Psychiatric Genomics Consortium, 2014. Biological insights from 108 schizophrenia-associated genetic loci. Nature 511, 421–427.

Schutyser, E., et al., 2003. The CC chemokine CCL20 and its receptor CCR6. Cytokine Growth Factor Rev. 14, 409–426.

Simonsen, C., et al., 2011. Neurocognitive dysfunction in bipolar and schizophrenia spectrum disorders depends on history of psychosis rather than diagnostic group. Schizophr. Bull. 37, 73–83.

Singhal, G., et al., 2014. Inflammasomes in neuroinflammation and changes in brain function: a focused review. Front. Neurosci. 8, 315.

Swanson, Karen V., Deng, Meng, Ting, Jenny P.-Y., 2019. The NLRP3 inflammasome: molecular activation and regulation to therapeutics. Nat. Rev. Immunol. 19 (8), 477–489. https://doi.org/10.1038/s41577-019-0165-0.

Tcw, J., et al., 2017. An efficient platform for astrocyte differentiation from human induced pluripotent stem cells. Stem Cell Rep. 9, 600–614.

Trajkovic, V., et al., 2004. Astrocyte-induced regulatory T cells mitigate CNS autoimmunity. Glia 47, 168–179.

Tran, N.N., et al., 2013. Modeling schizophrenia using induced pluripotent stem cell-derived and fibroblast-induced neurons. Schizophr. Bull. 39, 4–10.

Ulgen, E., 2018 et al. pathfindR: An R Package for Pathway Enrichment Analysis Utilizing Active Subnetworks. Preprint at bioRxiv DOI: https://doi.org/10.1101/272450.

Windrem, M.S., et al., 2017. Human iPSC glial mouse chimeras reveal glial contributions to schizophrenia. Cell Stem Cell 21, 195–208.e6.

Woiciechowsky, C., et al., 1999. Brain-IL-1beta induces local inflammation but systemic anti-inflammatory response through stimulation of both hypothalamic-pituitary-adrenal axis and sympathetic nervous system. Brain Res. 816, 563–571.

Zhang, N., et al., 2009. Regulatory T cells sequentially migrate from the site of tissue inflammation to the draining LN to suppress the alloimmune response. Immunity 30, 458–469.

Zhu, F., et al., 2018. Altered Serum Tumor Necrosis Factor and Interleukin-1β in First-Episode Drug-Naive and Chronic Schizophrenia. Front. Neurosci. 12, 296.